Experimental and theoretical spectral reflection properties of ice clouds generated in a laboratory chamber

Brian Barkey, K. N. Liou, Yoshihide Takano, and Werner Gellerman

In a preliminary experimental program, the measured bidirectional reflection properties between 1.0 and 3.5 μm from a grating spectrometer with a resolution of approximately 0.1 μm for ice crystal clouds generated in a cold chamber are compared with theoretical results computed from a line-by-line equivalent solar radiative transfer model. The theoretical calculations are based on the measured habits, concentrations, and sizes of the ice particles from replicas of the ice crystals that show a mean maximum size of approximately 7 μm. The experimental design was first tested with transmission measurements in a pure water-vapor environment that compare closely with theoretical expectations. Within the uncertainties and in consideration of the assumptions necessitated by the preliminary nature of this program, there is a close comparison between the experimental and theoretical results.

OCIS codes: 010.2940, 010.1310, 010.1290.

1. Introduction

In conjunction with the fundamental pursuit of determining the scattering and absorption characteristics of nonspherical ice crystals and the radiative properties of cirrus clouds, we initiated an experimental program to measure the reflection and transmission properties of ice crystal clouds generated in a laboratory cold chamber. The objectives of the present cloud spectroscopy experiments are twofold: to cross check the theoretical spectral radiative transfer and light-scattering programs developed for ice crystal clouds[1] with experimental results and to explore the information content of ice clouds that may not be available from the theory.

In line with these objectives, an apparatus was built to measure the spectral reflectance properties for ice crystal clouds generated in a cloud chamber. This experiment is similar to the one reported by Zander[2,3] more than 30 years ago. However, we place a stronger emphasis on determining the ice cloud microphysical properties so that a close and meaningful comparison can be carried out with theoretical results that are computed from a recently developed line-by-line equivalent solar radiative transfer model.[4] The experimental setup and the manner in which ice clouds are generated are first described, and then spectral reflectances that are determined from measurements and theoretical calculations are presented.

2. Experimental Setup

As shown in Fig. 1, the light from a 250-W tungsten–halogen lamp is sent through a diffraction grating monochromator which separates the light into wavelengths between 0.2 and 10 μm. The output from the monochromator is then collimated by a 13-cm spherical mirror and directed into the cloud chamber by another flat mirror. For transmission studies, the light is reflected back out of the chamber by a heated mirror at the chamber bottom and then focused onto a liquid-nitrogen-cooled indium antimonide detector by another 20-cm spherical mirror. With a preamplifier and phase-sensitive amplifier connected to this detector, it is possible to measure light from the tungsten–halogen lamp at a resolution of approximately 0.01 μm from 1.0 to 3.0 μm in the transmission mode. Note that the instrument noise contributes less than 0.1% uncertainty. To ensure the spectral accuracy of the experimental setup, the transmission properties of water vapor were measured as shown in Fig. 2. We determined this result

B. Barkey (barkey@bibbs.com), K. N. Liou, and Y. Takano are with the Department of Atmospheric Sciences, University of California, Los Angeles, Los Angeles, California 90095. W. Gellerman is with the Department of Physics, University of Utah, Salt Lake City, Utah 84112.

Received 21 July 1999; revised manuscript received 3 January 2000.

0003-6935/00/213561-04$15.00/0

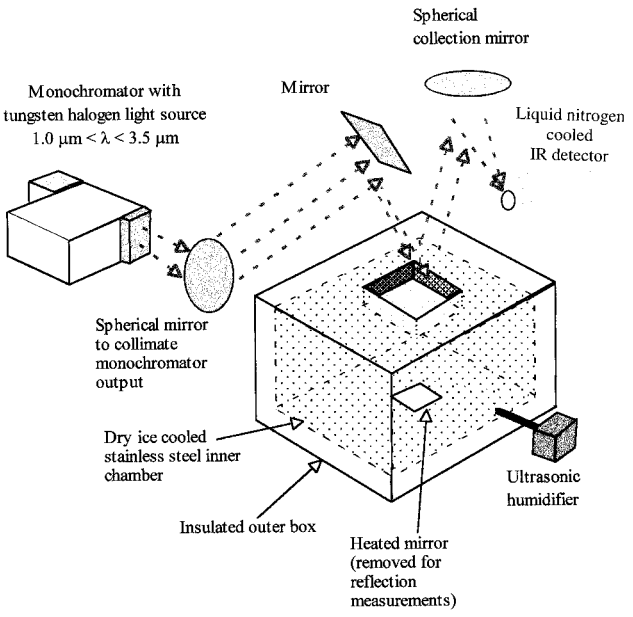

Fig. 1. Experimental setup used to measure the transmission properties of water vapor and the reflection properties of ice clouds. The chamber is cooled when dry ice is placed directly on top of the stainless-steel inner chamber.

by measuring the transmission signal through the moist chamber and then comparing it with a reference spectral signature that was taken from the chamber dried with compressed nitrogen gas to less than 20% relative humidity. The path length through the chamber was 1 m. Long-pass filters were used to reduce the effect of the multiple orders from the grating monochromator for this and other preliminary spectral results. Hence the results are the combination of a measurement from 1.0 to 2.0 μm, with a 1.0-μm long-pass filter, and a separate measurement from 2.0 to 3.0 μm, with a 2.0-μm long-pass filter. The water-vapor partial pressure is based on the measurements of the temperature (±2 °C) and relative humidity (±20%) from an electronic hygrometer thermometer.

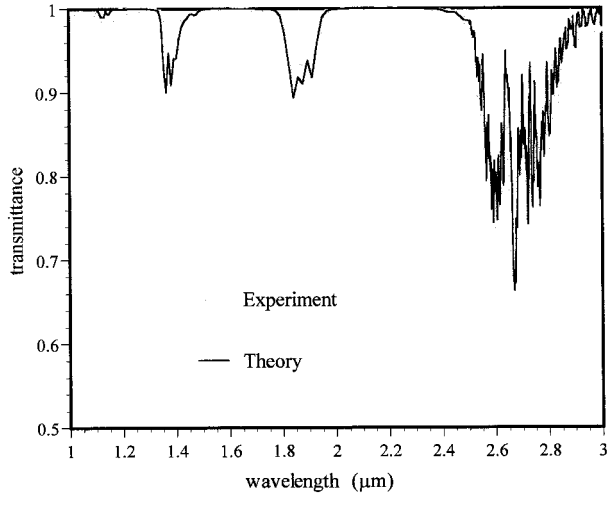

Fig. 2. Experimentally measured and theoretically derived water-vapor absorption properties.

The transmittance results shown in Fig. 2 are compared with those from theoretical calculations that we obtained using the measured water-vapor partial pressure of 34 ± 3 mbars, derived from the measured relative humidity of 83% at a temperature of 29 °C, as input to a spectral radiative transfer model based on the correlated k-distribution method.[5] These calculations are performed in the wave-number domain at a resolution of 50 cm^{-1} between 1 and 2.5 μm and at 1 cm^{-1} (averaged to match the experimental resolution of 0.01 μm) from 2.5 to 3 μm. Differences between the experimental and the theoretical results are less than 1% in the window regions and less than 5% in the band centers located at 1.1, 1.38, 1.87, and 2.7 μm. It is evident that the spectral position of the experimental features agrees closely with the expectation. The larger difference that can be seen between the theoretical and the experimental results at approximately 3 μm is due to the rapidly dropping intensity of the tungsten–halogen source past this wavelength.

3. Ice Cloud Development and Microphysics

The cloud chamber is a stainless-steel box 0.76 m by 0.76 m in width and 50 cm in height, and it is placed inside a larger, Styrofoam-insulated plywood box. The top of the inner box is removable for access to the inside and has a 25 cm by 30 cm hole through which light from the monochromator is directed. We cool the chamber by placing crushed dry ice around the steel box. The sensors from three electronic thermometers, accurate to ±2 °C, are placed near the top, at the middle, and at the bottom of the chamber in close proximity to the opening. Because of stratification, the temperature at the bottom of the chamber is usually less than that at the top by 5–6 °C; and because the cloud temperature is much lower than the room temperature, the ice cloud has a well-defined and relatively stable upper boundary at the chamber hole. Temperatures that are reported here are those recorded nearest the chamber hole at the top of the cloud. We can produce ice crystals by injecting small water droplets generated by an ultrasonic humidifier into the cold chamber through an insulated tube. At temperatures less than −41 °C, homogeneous ice crystal formation is assured; and because the walls of the chamber are directly cooled by the dry ice, a nucleating source is present even when the chamber temperature is above −41 °C. A thin cloud can be visually seen to persist in the box for approximately 10 min; and a thicker cloud, as determined visibly and from reflection and transmission measurements, must be maintained by our continuously pumping water droplets into the chamber to compensate for the loss of particles falling to the floor or diffusing onto the walls. Because the focus was on the reflection and transmission measurements at this point, no attempt was made to control the ice crystal habit or concentration. A diode laser (670 nm) and a silicon photodetector were placed within

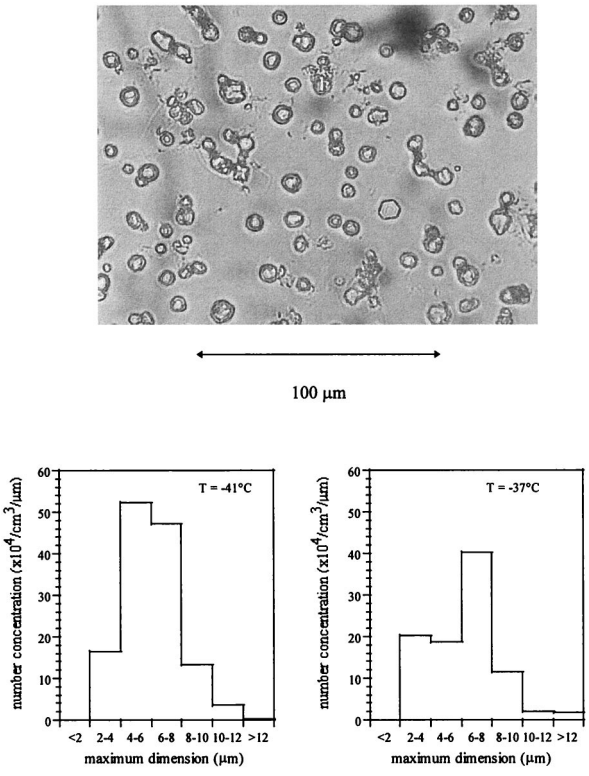

Fig. 3. Sample ice crystal particles replicated immediately after the reflectance measurement along with the ice particle size distribution derived from replicas taken before ($T = -41$ °C) and after ($T = -37$ °C) the reflection measurement.

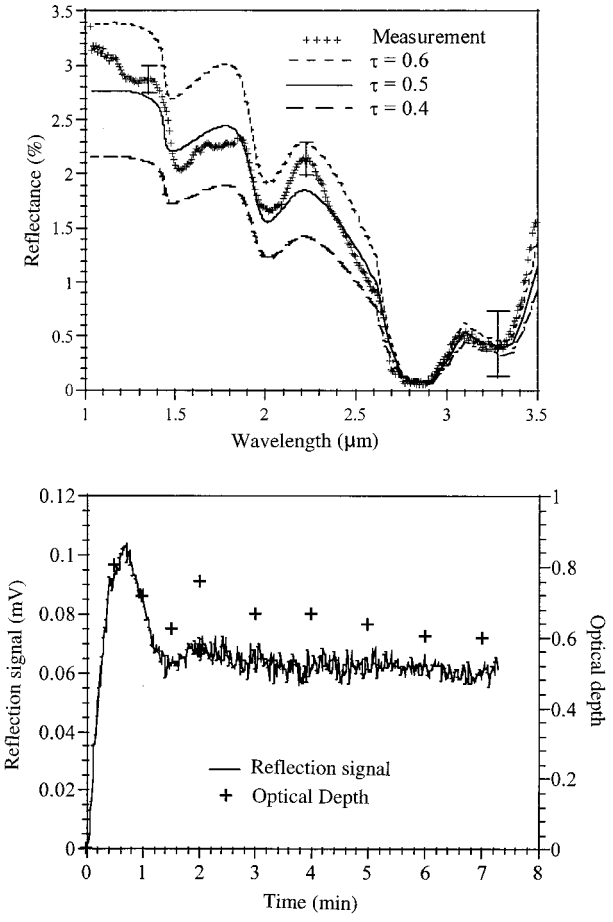

Fig. 4. Experimentally measured spectral reflection for incident light at 0° and detection at 22° from the vertical, along with theoretical expectations based on the measured microphysical properties of the ice cloud at three different optical depths, are shown in the upper plot. The lower plot shows the typical variability of the ice cloud as measured by the extinction of a laser beam and by a monochromatic reflection measurement that produces an uncertainty in the spectral result as indicated by error bars in the upper plot.

the chamber to monitor the ice cloud extinction properties near the chamber hole.

Just before and immediately after reflection measurements of the ice cloud are made, we form replicas of the cloud by allowing the ice crystals to fall onto a microscope slide coated with acrylic placed approximately 12 cm below the top of the cloud for a short time period of 3 ± 0.5 s. We then expose the slides to a relatively warm vapor of trichloroethylene in the manner described by Takahashi and Fukuta.[6] The solvent vapor allows the plastic substrate to flow up and over the ice crystals to form a hard permanent cast. Figure 3 shows a photomicrograph of a typical replica and the size distribution taken before ($T = -41$ °C) and after ($T = -37$ °C) the reflection measurement. The temperature in the chamber changes because of the continuous injection of water droplets during the spectral measurement. The ice cloud particle concentration is developed from the ice crystal size distribution counted from photomicrographs of the replicas—the particle terminal velocity based on the parameterization developed by Heymsfield and Kajikawa[7] for hexagonal plates—and the time of replicator exposure to the ice cloud. Extinction properties based on these concentrations and the particle projected area agree, within experimental uncertainties and assumptions, with the extinction of the laser beam through the ice cloud. Because this method does not characterize the ice cloud when reflectance measurements are taken, we are configuring a microscope video camera to measure the ice crystal sizes and shapes in a manner similar to that developed by Arnott *et al.*[8]

4. Ice Cloud Reflectance

The optical arrangement for reflection measurements, shown in Fig. 1, is exactly the same as that of the transmission measurements except that the heated mirror at the bottom of the chamber is removed. Because the reflected light intensity is considerably less than the direct beam used for transmission measurements, the intensity output of the monochromator is increased with a corresponding reduction in spectral resolution to approximately 0.1 μm. There is no detectable reflection signal without a cloud because the chamber walls are coated with a nonreflective paint. Shown in Fig. 4 is the result of our comparing the light reflected from the top of an ice cloud measured at an angle of 22° with the incident light at nadir to that of the same measurement

from a diffuse reflectance standard (IRT-94-100 from Labsphere Inc.) placed at the chamber opening. Also shown in Fig. 4 is a plot of the cloud density as measured by the extinction of a laser beam near the chamber hole and by the monochromatic reflection signal as a function of time. After the large spike in cloud density, caused by the initiation of water droplet injection, the cloud reflectance displays high-frequency oscillations that are caused by the turbulence of the continuous water droplet injection superimposed on a slower downward drift in the reflection signal. The effect of high-frequency variations in the reflection measurement is reduced by one's averaging three spectral reflection measurements taken in close succession which takes approximately 7 min, during which the monochromatic reflection signal can change up to 10%. Because the signal intensity retrieved over the spectrum is not constant, the percent error that is due to the turbulence in the final ratio is approximately 3–4% from 1 to 2 μm, approximately 5% from 2 to 2.6 μm, and between 10 and 20% above 2.6 μm. The maxima located at 1.3, 1.7, 2.2, and 3.1 μm are shown in the spectrum, along with minima at approximately 1.5 and 2.0 μm, which correspond to the absorption properties of bulk ice. The strong minimum at approximately 2.8 μm is associated with the Christiansen effect, which is caused by the real part of the refractive index going toward unity accompanied by an increase of absorption at this wavelength.

Using the line-by-line equivalent radiative transfer model[4] with an ice crystal mean effective size of 10 μm, we carried out a number of calculations. The model employs a combination of plate and other irregular crystals in the light-scattering and radiative transfer calculations.[1] The model assumptions are close to the ice crystal shapes that were seen in the replicas and to the mean crystal size (~7 μm) that was obtained in the experiment. The amount of water vapor in the cloud chamber was taken to be the saturation water vapor over ice at the chamber temperature. Because of uncertainties in the ice cloud microphysical determination, three optical depths of 0.4, 0.5, and 0.6 were used in the calculations. The spectral resolutions of the theoretical expectations, which are calculated in the wave-number domain, were approximately 0.3 μm for wavelengths less than 2.6 μm, and 0.05 μm for wavelengths above 2.6 μm. The theoretical points, which are not shown in Fig. 4, are connected by use of a spline fit. The optical depth of 0.5 appears to give the best match over the entire spectral interval, except in the vicinity of the 1.0- and 2.2-μm wavelengths.

5. Conclusion

A preliminary experimental setup has been constructed to measure the reflectance properties of an ice cloud. The optical characteristics of the system have been verified with measurements of water-vapor transmission properties. The experimentally measured bidirectional reflectance from an ice cloud compares reasonably well with theoretical results based on the measured ice crystal habits, concentrations, and sizes of the ice particles. Because of the preliminary nature of this study, there are uncertainties in the optical measurement associated with the highly variable cloud condition and in the assessment of the microphysical properties of the cloud. Considerable difficulties remain in matching the experimental and theoretical results in a precise manner. Future improvements will include temperature-controlled refrigeration of the cloud chamber and a continuous and concurrent method to determine the cloud microphysical properties and optical depth. Measurements of the reflectance properties at other wavelengths and use of a variety of incident and reflection geometries will be conducted in future experiments.

The authors are grateful to P. Sokolsky of the Department of Physics at the University of Utah for use of some of their equipment and for their advice on optics. Our thanks also go to N. Fukuta for assistance and advice with the cloud microphysical aspects of this research. This research was supported by National Science Foundation grants ATM-97-96277 and ATM-99-07924.

References

1. K. N. Liou, Y. Takano, and P. Yang, "Light scattering and radiative transfer in ice crystal clouds: applications to climate research," in *Light Scattering by Nonspherical Particles: Theory, Measurements, and Geophysical Applications*, M. I. Mischenko, J. W. Hovenier, and L. D. Travis eds. (Academic, New York, 2000), pp. 417–449.
2. R. Zander, "Spectral properties of ice clouds and hoarfrost," J. Geophys. Res. **71,** 375–378 (1966).
3. R. Zander, "Additional details on the near-infrared reflectivity of laboratory ice clouds," J. Geophys. Res. **73,** 6581–6584 (1968).
4. K. N. Liou, P. Yang, Y. Takano, K. Sassen, T. Charlock, and W. Arnott, "On the radiative properties of contrail cirrus," Geophys. Res. Lett. **8,** 1161–1164 (1998).
5. Q. Fu and K. N. Liou, "On the correlated k-distribution method for radiative transfer in nonhomogeneous atmospheres," J. Atmos. Sci. **49,** 2139–2156 (1992).
6. T. Takahashi and N. Fukuta, "Ice crystal replication with common plastic solutions," J. Atmos. Oceanic Technol. **5,** 129–135 (1988).
7. A. J. Heymsfield and M. Kajikawa, "An improved approach to calculating terminal velocities of plate like crystals and graupel," J. Atmos. Sci. **44,** 1088–1099 (1987).
8. W. P. Arnott, Y. Dong, and J. Hallet, "Extinction efficiency in the infrared (2–18 μm) of laboratory ice clouds: observations of scattering minima in the Christiansen bands of ice," Appl. Opt. **34,** 541–551 (1995).